
# AFRL-RH-WP-TR-2015-0070

## HOST-PATHOGEN COUPLED NETWORKS: MODEL FOR *BACILLUS ANTHRACIS* INTERACTION WITH HOST MACROPHAGES

**Peter J. Robinson**
**C. Eric Hack**
**Amanda L. Hanes**
**Emily J. Fleming**
**Jeffery M. Gearhart**
Henry M. Jackson Foundation
for the Advancement of Military Medicine
Wright-Patterson AFB OH

**Kyung O. Yu**
Bioeffects Division
Molecular Bioeffects Branch

September 2015

Final Report for October 2012 - September 2015



**Air Force Research Laboratory**
**711th Human Performance Wing**
**Human Effectiveness Directorate**
**Bioeffects Division**
**Molecular Bioeffects Branch**
**Wright-Patterson AFB OH 45433-5707**

# NOTICE AND SIGNATURE PAGE

Using Government drawings, specifications, or other data included in this document for any purpose other than Government procurement does not in any way obligate the U.S. Government. The fact that the Government formulated or supplied the drawings, specifications, or other data does not license the holder or any other person or corporation; or convey any rights or permission to manufacture, use, or sell any patented invention that may relate to them.

Qualified requestors may obtain copies of this report from the Defense Technical Information Center (DTIC) (http://www.dtic.mil).

The experiments reported were conducted according to the "Guide for the Care and Use of Laboratory Animals," Institute of Laboratory Animal Resources, National Research Council.

(AFRL-RH-WP-TR-2015-0070) has been reviewed and is approved for publication in accordance with assigned distribution statement.

YU.KYUNG.OH.1228570016
Digitally signed by YU.KYUNG.OH.1228570016
DN: c=US, o=U.S. Government, ou=DoD, ou=PKI, ou=USAF, cn=YU.KYUNG.OH.1228570016
Date: 2015.11.16 12:03:36 -05'00'

KYUNG O. YU
Work Unit Manager
Molecular Bioeffects Branch

MILLER.STEPHANIE.A.1230536283
Digitally signed by MILLER.STEPHANIE.A.1230536283
DN: c=US, o=U.S. Government, ou=DoD, ou=PKI, ou=USAF, cn=MILLER.STEPHANIE.A.1230536283
Date: 2015.11.17 21:06:05 -06'00'

STEPHANIE A. MILLER, DR-IV, DAF
Chief, Bioeffects Division Human Effectiveness Directorate 711th Human Performance Wing
Air Force Research Laboratory

This report is published in the interest of scientific and technical information exchange, and its publication does not constitute the Government’s approval or disapproval of its ideas or findings.

# REPORT DOCUMENTATION PAGE

*Form Approved*
*OMB No. 0704-0188*



| 1. REPORT DATE *(DD-MM-YYYY)* | 2. REPORT TYPE | 3. DATES COVERED *(From - To)* |
|---|---|---|
| 30-09-2015 | Final | Oct 2012 – Sept. 2015 |

**4. TITLE AND SUBTITLE**
Host-Pathogen Coupled Networks: Model for *Bacillus anthracis* Interaction with Host Macrophages

**5a. CONTRACT NUMBER**
In-House

**5b. GRANT NUMBER**
NA

**5c. PROGRAM ELEMENT NUMBER**
62202F

**6. AUTHOR(S)**
Robinson, Peter J.[1]; Hack, C. Eric[1]; Hanes, Amanda L.[1]; Fleming, Emily J.[1]; Gearhart, Jeffery M.[1]; Yu, Kyung O.*

**5d. PROJECT NUMBER**
ODTW

**5e. TASK NUMBER**
P0

**5f. WORK UNIT NUMBER**
05/H069

**7. PERFORMING ORGANIZATION NAME(S) AND ADDRESS(ES)**
[1]HJF, 2729 R St, Bldg 837, WPAFB OH 45433-5707

**8. PERFORMING ORGANIZATION REPORT NUMBER**

**9. SPONSORING/MONITORING AGENCY NAME(S) AND ADDRESS(ES)**
Air Force Materiel Command*
Air Force Research Laboratory
711th Human Performance Wing
Human Effectiveness Directorate
Bioeffects Division
Molecular Bioeffects Branch
Wright-Patterson AFB OH 45433-5707

**10. SPONSOR/MONITOR'S ACRONYM(S)**
711 HPW/RHDJ

**11. SPONSORING/MONITORING AGENCY REPORT NUMBER**

**12. DISTRIBUTION AVAILABILITY STATEMENT**
Distribution A: Approved for public release; distribution unlimited. (PA Case No. 88ABW-2015-5572. Date 12 November 2015.

**13. SUPPLEMENTARY NOTES**

**14. ABSTRACT**
Macrophages are key in establishing *Bacillus anthracis* (BA) infection via spore germination, and providing transportation to the regional lymph nodes where vegetative BA bacteria synthesize protective antigen (PA), lethal factor (LF), and edema factor (EF) for release into circulation. PA binds to anthrax toxin receptors on the endosomal membrane to form oligomeric pores that mediate transport of LF (and EF) into the cytosol, where it accumulates, causing macrophage death and the release of accumulated toxins and bacteria. We describe an *in silico* quantitative model of cytosolic LF attacking the host cell's mitogen-activated protein kinase (MAPK) signaling pathway that includes the time-course of LF accumulation in the cytosol, and LF-mediated cleavage of MAPK kinases in terms of a second order rate constant. Cytosolic LF accumulation is determined by external LF and PA concentrations via a composite Hill-type equation. Additional key parameters include total numbers of macrophage ATR/TEM8 or $CMG_2$ ($ANTR_{1/2}$) receptors for pore formation by PA; LF flux into cytosol through each such pore; binding affinities of PA (to surface receptors) and LF (to pores); and cytosolic LF half-life. Sensitivity analysis shows that LF half-life is critical to the sensitivity of AKR, BL/6, DBA and human macrophages to LF (with their viability half-lives of 48 to 72 hours *in vitro*), but not the RAW264.7, J774A.1 or BALB/C macrophages having shorter half-lives of 1-3 hours, where macrophage viability is primarily determined by LF influx into the cytosol. The model forms a link between multi-cellular organism-level infection models, and sub-cellular molecular pathway models.

**15. SUBJECT TERMS**
mathematical model, signaling pathways, bacterial infection, macrophage, immune system, *Bacillus anthracis*, anthrax

| 16. SECURITY CLASSIFICATION OF: | | | 17. LIMITATION OF ABSTRACT | 18. NUMBER OF PAGES | 19a. NAME OF RESPONSIBLE PERSON |
|---|---|---|---|---|---|
| | | | | | K. O. Yu |
| a. REPORT | b. ABSTRACT | c. THIS PAGE | | | 19b. TELEPONE NUMBER (*Include area code*) |
| U | U | U | SAR | 36 | NA |

Standard Form 298 (Rev. 8-98)
Prescribed by ANSI-Std Z39-18

THIS PAGE INTENTIONALLY LEFT BLANK.

## TABLE OF CONTENTS

## LIST OF FIGURES

## LIST OF TABLES

THIS PAGE INTENTIONALLY LEFT BLANK.

## PREFACE

Funding for this project was provided through the Defense Threat Research Agency (DTRA) under award number CBS.MEDBIO.03.10.AHB.007. This research was conducted under cooperative agreement FA8650-10-2-6062 with the Henry M. Jackson Foundation for the Advancement of Military Medicine (HJF). The program manager for the HJF contract was David R. Mattie, PhD (711 HPW/RHDJ, formerly AFRL/RHPB), who was also the technical manager for this project.

The authors would like to thank Dr. Dan Wolfe (DTRA) for financial support and valuable discussions. The authors acknowledge John J. Schlager, PhD (711 HPW/RHD) for his assistance with funding submissions and research focus. The authors also would like to acknowledge Teresa R. Sterner of HJF (Wright-Patterson AFB OH) for formatting this technical report for submission.

THIS PAGE INTENTIONALLY LEFT BLANK.

## 1.0 SUMMARY

The present model describes aspects of the interaction between *Bacillus anthracis* (BA) and the early responder cells, the alveolar macrophages of the host immune system. As such, it provides a framework for understanding the impact of anthrax on the host system and how the host system's defense mechanisms are disrupted for the benefit of the invading organism. Macrophages are key in the establishment of BA infection via spore germination, and providing transportation to the regional lymph nodes where vegetative *B. anthracis* bacteria synthesize protective antigen (PA), lethal factor (LF), and edema factor (EF) for release into the circulation.

For simplicity, we have developed the model to describe a situation for which *in vitro* data is available, in which macrophages of various types are exposed to specific concentrations of LF and PA. Under such circumstances, PA binds anthrax toxin receptors on the endosomal membrane to form oligomeric pores that mediate the transport of LF (and EF) into the cytosol, where it accumulates, causing macrophage death and the release of accumulated toxins and bacteria. Cell death is caused by cytosolic LF attacking the host cell's mitogen-activated protein kinase (MAPK) signaling pathway by cleavage of MAPK kinases. The model describes quantitatively the time-course of LF accumulation in the cytosol, and LF-mediated cleavage of MAPK kinases in terms of a second order rate constant. Cytosolic LF accumulation is determined by external LF and PA concentrations via a composite Hill-type equation (1910) that incorporates pore formation and transport of LF through those pores from the external medium into the cytosol.

Additional key parameters include:

- Total numbers of macrophage ATR/TEM8 or CMG2 (ANTR1/2) receptors for heptameric pore formation by PA;
- LF flux into cytosol through each such pore;
- Binding affinities of PA (to surface receptors) and LF (to pores); and
- Cytosolic LF half-life.

Sensitivity analysis of the model shows that LF half-life is critical to the sensitivity of AKR, BL/6, DBA and human macrophages to LF (with their viability half-lives of 48-72 hours *in vitro*), but not the RAW264.7, J774A.1 or BALB/C macrophages having shorter half-lives of 1-3 hours, where macrophage viability is primarily determined by LF influx into the cytosol.

By mechanistically describing LF-dependent macrophage viability, bacterial death and production of cytokines that recruit additional immune cells and modulate the immune response, the model forms a link between organism-level models of *B. anthracis* infection that describe bacterial proliferation in the host (and the host's immune response), and molecular-level models describing the subversion of the molecular machinery of the immune cells themselves.

## 2.0 INTRODUCTION

*Bacillus anthracis* (BA) is a Category A Select Agent that causes fatal systemic disease in animals and humans known as anthrax following a primary pneumonic exposure (Glassman, 1966). As with most bacteria deposited in the deep lung, *B. anthracis* interacts with toll-like receptors (TLRs) at the surface of host macrophages, triggering endocytosis and up-regulation of various signaling pathways in the macrophage in order to both neutralize the spore/bacterium and initiate a wider immune response to the infection. Both mitogen-activated protein kinases (MAPK) and NF-kB pathways are involved in cytokine production and release (Figure 1). Both pathways also promote macrophage survival by up-regulating inhibition of apoptosis (Zhang *et al.*, 2005). Rather than via the anti-inflammatory apoptotic pathway, host cell death may result from pyroptosis. This caspase-1 dependent pathway also results in the production and release of pro-inflammatory cytokines such as IL-1B and IL-18 (Fink and Cookson, 2005), potentially initiating a wider immune response. In addition, the NF-kB pathway is involved in the neutralization of the pathogen via nitric oxide (NO) delivered by lysosomal fusion (Jones *et al.*, 2007).

In response, pathogens may counteract host cell strategies by interfering with host cell defensive processes, and thus provide a favorable intracellular environment for themselves for survival and initial proliferation. Once within the acidic environment of the endosome, the *B. anthracis* spore germinates as it is transported to the regional lymph node where it ultimately escapes into the circulation. The vegetative *B. anthracis* begins to produce the three (separately non-toxic) proteins to which *B. anthracis* owes its virulence. These proteins are protective antigen (PA), lethal factor (LF), and edema factor (EF). LF is a metalloprotease that cleaves most isoforms of MAPK kinases (MAPKKs) close to their N-terminus (Duesbery *et al.*, 1998; Vitale *et al.*, 1998), while EF acts as a calcium anion and calmodulin dependent adenylatecyclase that greatly increases the level of cyclic adenosine monophosphate (cyclic AMP) in the cell. LF and EF toxicity is dependent on PA, which binds to the host cell membrane and upon heptamerization (or octamerization, Kintzer *et al.*, 2009), shuttles LF and/or EF into the host cell's cytosol where they modulate the MAPK and other pathways, and cyclic AMP synthesis, respectively, ultimately leading to systemic shock. The mixture of LF and PA produced by BA is known as lethal toxin (LeTx), while that of EF and PA is known as edema toxin (EdTx).

The toxemia that ensues following systemic *B. anthracis* infection has been well characterized (Dixon *et al.*, 1999), with cardiomycocytes and vascular smooth muscle cells being critical target cells for lethal toxin mediated host death (Liu *et al.*, 2013). However, the role of toxins in the early stages of *B. anthracis* infection remains somewhat controversial. Nonetheless, this early interaction between the pathogens and the host's first responder cells determines the survival and initial proliferation of the pathogen, and sets the stage for the subsequent course of the infection. Studies by Guidi-Rontani (2002) have shown that germination of spores within alveolar macrophages is closely followed by toxin gene expression, and that the survival of germinated spores and the death of macrophages were associated with toxin gene expression. Further, the effects of LeTx on macrophage cytolysis may be due to LeTx accumulation, overloading, and diffusion of toxic effectors. LeTx modulation of the oxidative burst leads to overproduction of reactive oxygen species and reactive nitrogen intermediates (due to MAPKK cleavage) which are toxic when they reach the cell's cytosol (Guidi-Rontani, 2002). They further speculate that

germinated spores express virulence factors that exhibit phagolysosome membrane-damaging activity leading to the release of bacteria to the macrophage cytosol. From Banks *et al.* (2005): "There is conflicting evidence regarding whether or not expression of LeTx and EdTx are required for survival and escape of the germinated *B. anthracis* spore from the lysosome and whether or not vegetative bacilli replicate in the macrophage cytosol."

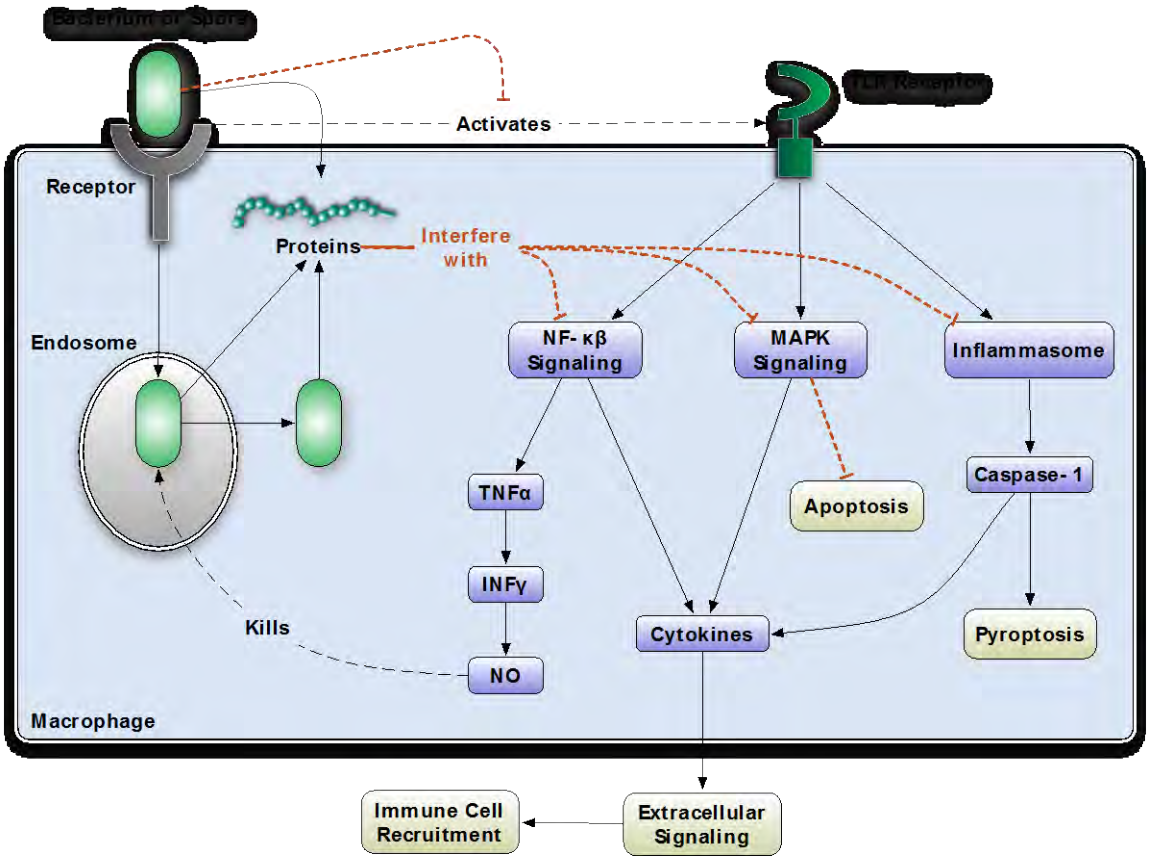


**Figure 1. General Schematic of the Initial Interaction of a Bacterium and Macrophage, Leading to Endocytosis of the Bacterium or Spore, and the Activation of a Series of Signaling Pathways in the Macrophage.** These signaling cascades are designed to trigger a number of adaptive responses in the macrophage, including those required to kill the endocytosed bacterium, and those needed to produce cytokine signals to recruit other immune cells.

Regardless of the stage of infection, LF (and EF) must be delivered to the host cell cytosol in order to disrupt cell signaling processes. PA plays an essential role in the delivery of both LF and EF into the cytosol, and is the primary reason for the non-lethality of LF (and EF) alone. This process is presumed to be the same as occurs in the latter part of the interaction between PA and other cells of the body later in an infection (see Figure 2). When encountering a cell-surface receptor from the systemic circulation, PA is cleaved into two fragments by a furin-like protease.

The amino-terminal fragment, [PA20], dissociates into the medium, and this allows the carboxy-terminal fragment, [PA63], to heptamerize and to bind LF (and EF). Krantz *et al.* (2006) have shown that each such heptamer can bind up to three molecules of LF and/or EF. The resulting complexes of [PA63]7 and LF (and EF) are taken up into cells by receptor-mediated endocytosis and moved to a low-pH endosomal compartment. There, the acidic environment induces a conformational change in the [PA63]7 heptamer that allows it to insert into the membrane and form a pore. This conversion promotes the translocation of bound LF (and EF) across the endosomal membrane to the cytosol (Figure 2).

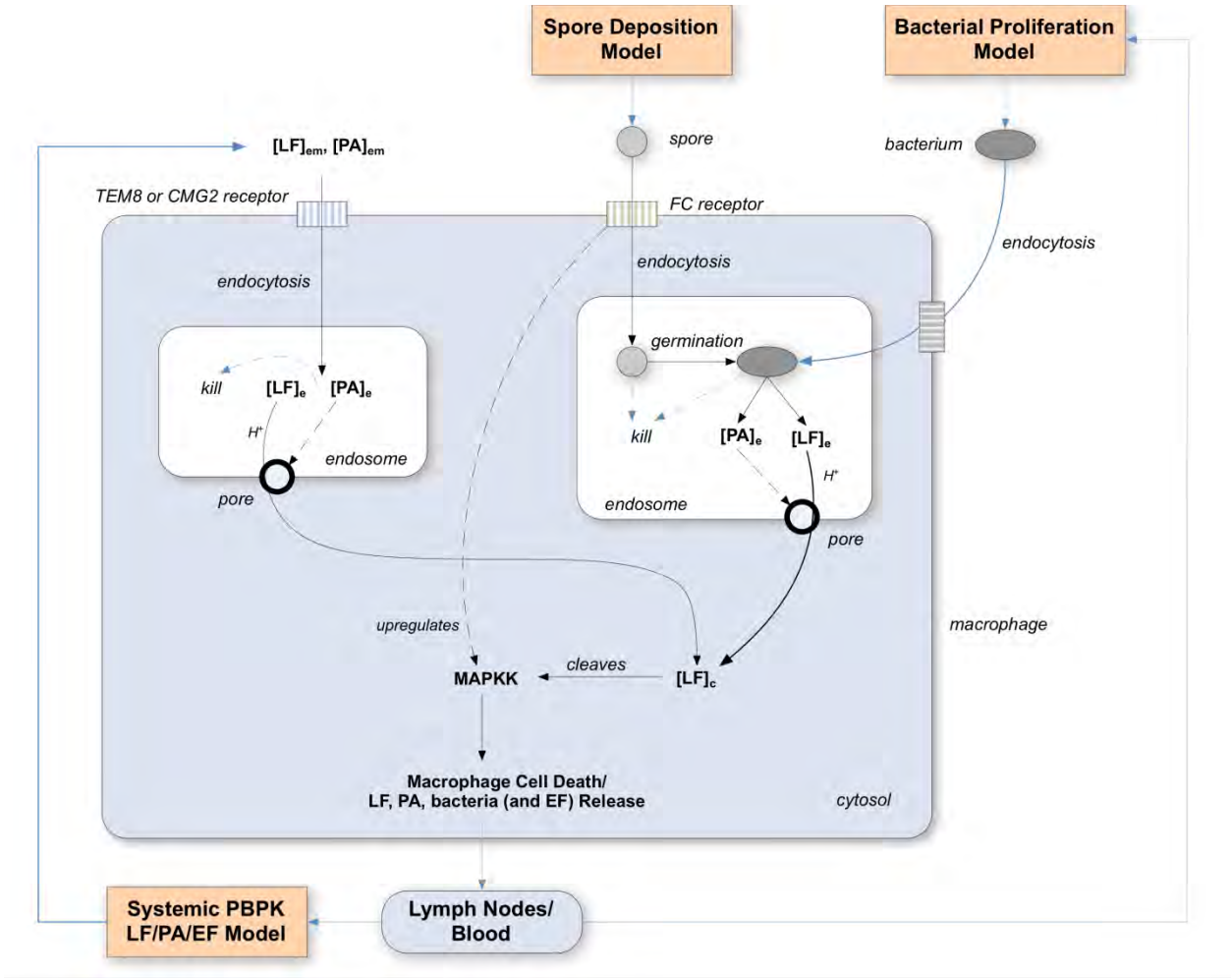


**Figure 2. Simplified Schematic of the Interaction of *B. anthracis* with Macrophages, Culminating in the Disruption of the MAPK Signaling Pathway by LF in the Cytosol, Cell Death and Bacteria/Toxin Release** (from Robinson *et al.*, 2010)

Such current understanding of the multi-faceted interactions between a host organism and a potentially virulent invading bacterium can be integrated into a mechanism based, validated and quantitative computational model of the processes involved. Such a model, developed in an

extensively studied host species, can be extrapolated to other species and conditions of interest by appropriate modification of key parameters and other components of the model. Effective prognosis and intervention strategies depend on having a predictive model of bacterial proliferation and the host's immune response that is sensitive to both the initial exposure conditions (number of bacteria inhaled/ingested, etc.) and the state of the host's immune system as it is ramped up in response to the pathogen. The initial development of such a model is clearly a very data-intensive process and involves a detailed understanding of the mechanisms involved on multiple levels of organization, from the molecular and cellular levels, up to the level of the whole organism, and beyond to the responses of populations of varied individuals.

The mechanisms of *B. anthracis* virulence are well characterized (see above), and we are developing *in silico* models of anthrax on multiple host physiological levels in order to predict the regional deposition of *B. anthracis* spores in the lungs of animals and humans, the phagocytosis and transport of spores by alveolar macrophages, the death of infected macrophages and release of bacteria and toxins into circulation, and the bacteremia and toxemia that ultimately lead to the demise of the host. A number of computational models have been developed that hone in on specific, important aspects of *B. anthracis* virulence in order to deepen the understanding of mechanisms of pathogenesis and immune subversion and its impact on pathogen proliferation (e.g., Gutting *et al.*, 2008; Kumar *et al.*, 2008; Day *et al.*, 2011), but few aim to quantify human dose response by taking a multi-scale approach. We have already described an initial model for the interaction of LF with the macrophage's MAPK signaling pathway (Robinson *et al.*, 2010). Here we extend this model to include the PA-dependent accumulation of LF in the cytosol of the macrophage. Such an extended model is necessary for a number of reasons. Our kinetic model for LF accumulation in the cytosol of host macrophages puts the cellular signaling model in an *in vivo* context, in which, depending on its location and the stage of progression of the infection, the macrophage is exposed to spores, bacteria, as well as circulating LF and PA. In addition, we will ultimately be able to use our model to describe and predict the efficacy of therapies that focus on PA (as well as LF).

## 3.0 METHODS

### 3.1 Model for MAPK Kinase (MAPKK) Cleavage by LF

In a previous paper (Robinson *et al.*, 2010), we outlined a mathematical model for the interaction of LF with the MAPK signaling pathway of host macrophages. Our representation of the MAPK pathway was based on the model of Kholodenko (2000), which we modify and develop to take into account the effect of disruption by BA (Figure 3). The interaction of BA with this pathway was assumed to take place via cleavage of the three MAPK kinases (MAPKK, unphosphorylated and phosphorylated) by BA derived LF in the cytosol of the macrophage, as represented by the red arrows in Figure 3. Each cleavage process was assumed to be first-order, with its reaction rate JX (nM $s^{-1}$) proportional to each respective MAPKK concentration, MKK, MKK_P and MKK_PP (nM), as shown in Equation Set 1:

$$JX = KX*MKK$$

$$JXP = KXP*MKK\_P$$ .....Equation Set 1
$$JXPP = KXPP*MKK\_PP$$

We assumed that these rate constants are all equal: KX=KXP=KXPP ($s^{-1}$). Since this cleavage process was assumed to be the primary cause of macrophage cell death when exposed to LeTx, we fitted numerical values of KX (=KXP=KXPP) to *in vitro* cell viability data for various macrophage strains, and thereby quantified their differential susceptibilities to LeTx (and by implication, to BA itself) (see Table 2 in the Results below).

In reality, however, each of these reaction rates are second-order, since they are also proportional to the local concentration of LF in the cytosol of the macrophage, LFC (also expressed as LFc). Thus Equation Set 1 becomes:

$$JX = KX2*LFC*MKK$$
$$JXP = KX2*LFC*MKK\_P$$ .....Equation Set 2
$$JXPP = KX2*LFC*MKK\_PP$$

…, where now *KX2* is a second-order cleavage rate constant with units of, for example, $nM^{-1}s^{-1}$.

In general, $LF_c$ is the result of LF accumulation from a number of sources in the infected organism (see Figure 2 above), is dependent on its state of infection, and is not generally known. In the present paper we consider, for model development and validation purposes, a special case in which $LF_c$ may be more readily inferred. A number of *in vitro* studies have been conducted (Pellizzari *et al.*, 1999; Muehlbauer *et al.*, 2007) in which specific macrophage cell types were directly exposed to LF and PA at specific external concentrations $LF_e$ and $PA_e$, which will determine $LF_c$ in a more direct manner than the more complex *in vivo* situation. In many ways, this *in vitro* situation is similar to later stages of infection when the primary source of LeTx is from circulating pools of the proteins, rather than directly from the bacteria themselves. Under these circumstances, delivery of LF to cytosol involves a number of sequential steps and sub-steps (Young and Collier, 2007):

- The 83 kDa form pf PA ($PA_{83}$) binds to receptor (ANTR1/2 plus LRP6 co-receptor)
- Proteolytically activated (cleaved) by furin (cellular protease) - removes a 20-kDa fragment [$PA_{20}$] from the N terminus, leaving the complementary 63-kDa fragment [$PA_{63}$] bound to the receptor
- Receptor-bound [PA63] then self-associates to form a ring-shaped heptameric (or octameric) complex - the prepore
- Prepore binds up to three molecules of LF and/or EF competitively
- Complex is endocytosed
- Prepore forms a pore in endosomal membrane (driven by low pH)
- LF unfolds and passes through this pore into the cytosol, and refolds

This process is illustrated in Figure 4, and forms the basis for the mathematical description that follows.

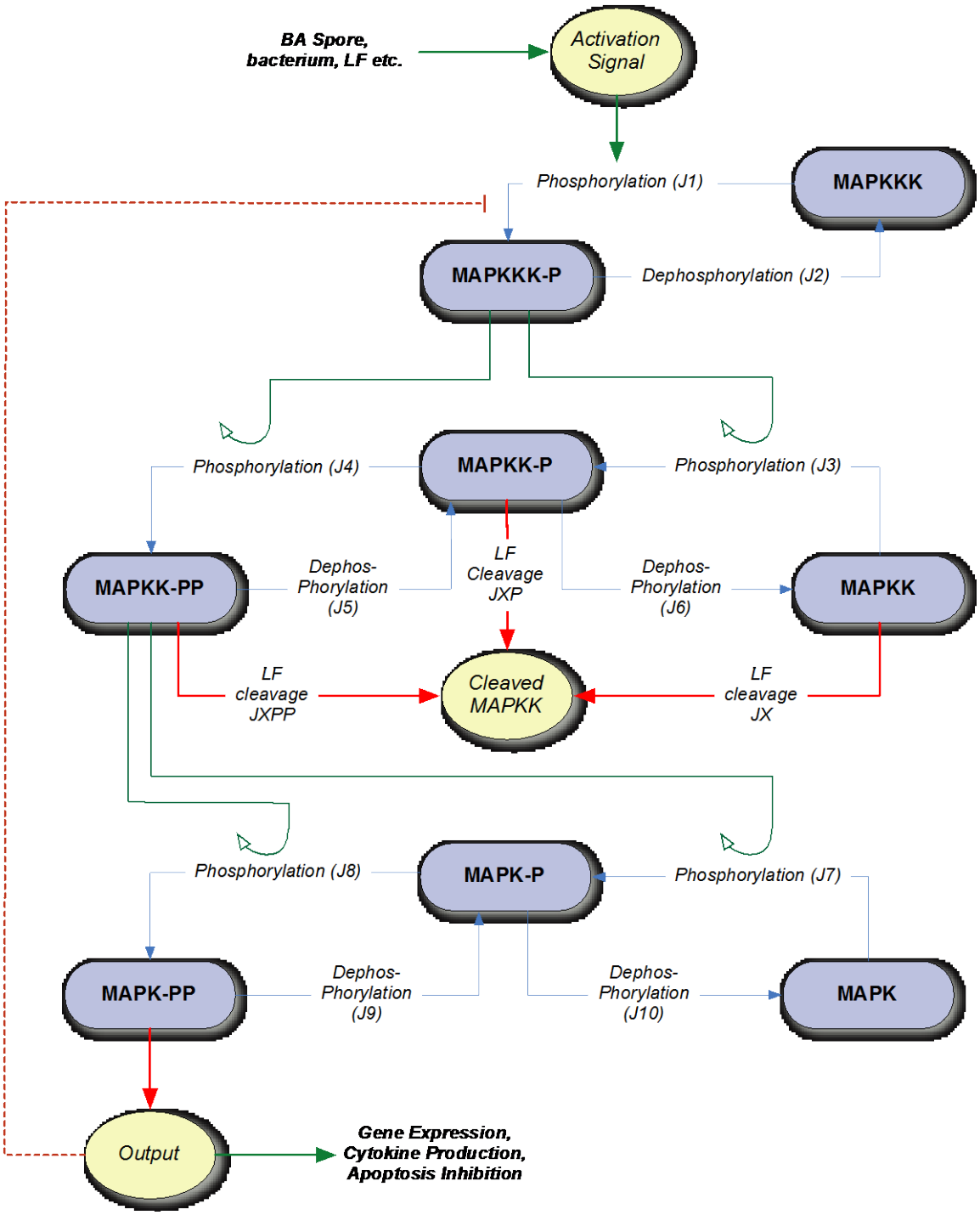


**Figure 3. Model Graph, from Kholodenko (2000), Adapted from BioModels Repository, European Bioinformatics Institute (EMBL-EBI).** This graphic illustrates the MAPK signaling cascade model as applied to the interaction with *B. anthracis*. Equations for the phosphorylation/dephosphorylation rates J1 through J10 are given in Robinson *et al.* (2010). The cleavage rates JX, JXP and JXPP by anthrax LF are given respectively by the products of

KX and the concentrations of MAPKK, MAPKKP and MAPKKPP (red arrows; Equation Set 2 in text). In Robinson *et al.* (2010), KX was assumed to be a first order rate constant. Here we include their dependence on local cytosolic LF concentrations, and KX becomes a second-order constant, KX2. Circles at the end of connectors indicate inhibition.

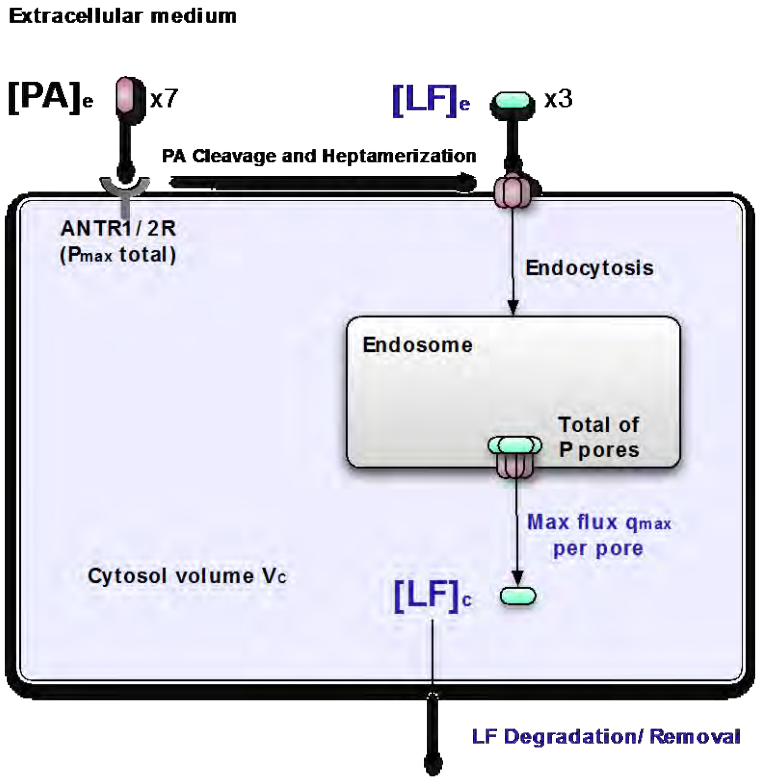


**Figure 4. Schematic Representation of Transport of LF from Extracellular Medium into the Cytosol of the Macrophage.** Subscript e represents the extracellular medium; c represents cytosol.

The number of heptameric pores, *P*, formed on the cell surface from PA ultimately determines the transport rate of LF from the medium into the cytosol. This number is in turn dependent on the PA concentration $PA_e$ in the medium, with an inherent maximum $P_{max}$, determined by the total number of ATR/TEM8 or CMG2 (ANTR1/2) receptors on the macrophage surface (Scobie and Young, 2005).

Suppose that a number *n* (in this case 7 or 8) PA units combine with the receptor so rapidly that all intermediate states between the unoccupied and fully occupied receptor can be neglected (Segel, 1980). Then we have:

$$P_o + n\,PA_e \overset{k_{on},\,k_{off}}{\longleftrightarrow} P, \quad \rightarrow \quad P_o + P = P_{max} \qquad \text{Equation 3}$$

…, where $P_0$ is the number of unoccupied receptors. In the steady-state we have:

$$k_{off}P = k_{on}P_0(PA_e)^n \quad \text{Equation 4}$$

…, which, on rearrangement, becomes the familiar Hill (1910) equation with coefficient, *n*:

$$P = \frac{(PA_e)^n P_{max}}{(PA_e)^n + K_m^{PA}} \quad \text{Equation 5}$$

Here $K_m^{PA}$ (= $k_{off}/k_{on}$) relates actual pore formation to PA concentration. When $PA_e = (K_m^{PA})^{1/n}$, half the maximum number of pores are created. The process of pore formation is of course complex, but Equation 5 captures the essence of this process for reasonable mathematical simulations.

Once these PA heptamers are formed, they may bind up to three LF (or EF) molecules (Collier, 2009), and endocytosis of the pore complex occurs. The LF molecules are then transported (translocated) through the pore into the cytosol. The ability of the pores to transport LF, and hence the maximum flux, $q_{max}$, is dependent on the (low) pH in the endosome (Krantz *et al.*, 2006). An alternative mechanism has been proposed for translocation of LF from the endosome into the cytosol, which involves the disruption of the endosomal membrane (Nablo *et al.*, 2013); if this were the case, our model would still apply, except $q_{max}$ would have an interpretation in the model related to a membrane "dissolution rate".

We assume that the total transport rate (flux), *TR* (nmol/s) of LF through the combined binding/endocytosis/pore translocation process for each of the *P* pores is driven by the LF concentration in the medium, and follows saturation kinetics with an effective maximum flux rate per pore of $q_{max}$ (nmol/s) and a total maximum flux of $P^*q_{max}$:

$$TR = \frac{P_{max}q_{max}(PA_e)^n(LF_e)^m}{((PA_e)^n + K_m^{PA})\,((LF_e)^m + K_m^{LF})} \quad \text{Equation 6}$$

Equation 6 thus links the cytosolic LF concentration, $LF_c$, (which drives the breakdown of the MAPK signaling pathway in terms of the present model) with the concentrations of LF and PA in the medium.

To ensure that the Cytosolic LF concentration does not continue to rise indefinitely as a result of influx from the external medium, we assume that there is some breakdown of LF in the cytosol or leakage into the surrounding media, so that the net change in LF concentration (in the absence of cleavage) is given by:

$$V_c \frac{d(LF_c)}{dt} = TR - k_{deg}LF_c \quad \text{Equation 7}$$

where $V_c$ is the volume of the cytosol compartment, and where $k_{deg}$ is the degradation or leakage rate constant ($s^{-1}$).

### 3.2 Parameter Estimates

Parameters for the MAPK model are taken directly from Kholodenko (2000) (see Table 1 below). Additional parameters and their units are also given in Table 1.

The degradation or leakage rate constant of LF from the cytosol is given in terms of the half-life *TH* (s or h) of LF in the cytosol as $k_{deg} = \ln 2/TH$. Extensive studies by Gupta *et al.* (2008) suggest that 'N-end rule'', which relates the half-life of proteins in cells to the identity of their N-terminal residue, applies to LF, so that the N-terminal residue of LF would determine the cytosolic stability and thereby the potency of LF. To support this hypothesis they measured cytosolic half-lives and potencies of a number of modified LF proteins. The half-life for LF-A was estimated to be 4.4 h ($1.6 \times 10^4$ s), so $k_{deg} = 4.4 \times 10^{-5}$ $s^{-1}$.

The number of PA binding sites $P_{max}$ per cell typically ranges from 2600 to 240,000, depending on cell type (Abi-Habib, 2005; Fleming *et al.*, 2009). Such a large variation of almost two orders of magnitude for different cell types indicates that this parameter is likely to be a major source of uncertainty unless it is measured for the particular cell type under consideration. Cytosol volume is about 70 percent of the total macrophage volume (Luby-Phelps, 2000). The maximum flux $q_{max}$ of LF through each pore is largely unknown. However, the contribution of the parameters $P_{max}$, $q_{max}$ *and* $V_c$ to the cytosolic LF concentration is mediated only through the ratio $R = (P_{max}q_{max})/V_c$ (units $nmol\ s^{-1}L^{-1} = nM\ s^{-1}$). Therefore, we really need to determine (or fit) only a value for the ratio $R$ for a specific total number of macrophages. (Once $R$ is fit in this way, $P_{max}q_{max}$ can be determined by estimating $V_c$).

The binding affinities $K_m$ for PA and LF are taken from the literature (Elliott *et al.*, 2000; Wigelsworth *et al.*, 2004; Wei *et al.*, 2006) (see Table 1) and show a wide variation dependent on the measurement methodology and cell/receptor preparation used. Specifically, Wei *et al.* (2006) looked at viability of M2182 human prostate carcinoma cells (with excess FP59 toxin) as well as RAW264.7 mouse macrophages (with excess LF) at various PA concentrations and typically observed 50 percent viability at around 0.01 nM. Wigelsworth *et al.* (2004) measured association and dissociation rates of PA with the CMG2 receptor and estimated the affinity to be 0.4 +/- 0.2 nM. Elliott *et al.* (2000) estimated dissociation constants for LF binding to PA63 heptamers to be 2.8 ± 0.8 nM (amine coupled PA), 11 ± 0.7 nM (Ni[$2^+$]nitrilotriacetate -coupled PA) and 0.4 nM (L6 cells).

Finally, we assume that the Hill (1910) or co-operativity coefficients $n$ and $m$ are 7 and 3 respectively. The external concentrations $PA_e$ and $LF_e$ are assumed to be the same as their respective concentrations in the bathing medium in the various *in vitro* studies we simulate below.

There are thus only two measured parameters ($K_m^{LF}$, $K_m^{PA}$), and two that are largely unknown (*KX2, R*) that can be estimated by fitting the current model to the cell viability data.

## Table 1: Model Parameters and Their Initial Values

| Parameter | Alternate symbol | Value | Units | Source | Description |
|---|---|---|---|---|---|
| *Pore transport:* | | | | | |
| $P_{max}$ | PMAX | Fitted: see Results | - | | # receptor sites (max # pores) |
| $q_{max}$ | QMAX | | nmol/s | | Transport rate per pore |
| $V_c$ | | | L | | Cytosol volume |
| $PA_e$ | PAE | From data | nM | | External PA concentration |
| $LF_e$ | LFE | | nM | | External LF concentration |
| $K_m^{PA}$ | KMD | ~0.01; 0.4±0.2 | nM | Wei, 2006; Wiglesworth 2004 | Michaelis const. for heptamer formation |
| $K_m^{LF}$ | KM | 0.4 to 11 | nM | Elliott, 2000 | Michaelis const. for pore LF transport |
| n | m | 7 | - | Hill coefficient | Hill coefficient for heptamer formation |
| m | mm | 3 | - | Hill coefficient | Hill coefficient for LF transport |
| $k_{deg}$ | | $4.4 \times 10^{-5}$ | $s^{-1}$ | Gupta et al., 2008 | LF degradation rate in cytosol |
| *MAPK Pathway:* | | | | | |
| KX2 | | Fitted: see Results | $nM^{-1}.s^{-1}$ | | 2nd order cleavage rate constant |
| V1 | $V_1$ | 2.5 | $nM^{-1}.s^{-1}$ | Kholodenko, 2000 | Maximal enzyme rate |
| Ki | $K_i$ | 9 | nM | " | Michaelis constant |
| n | | 1 | - | " | Negative feedback strength |
| K1 | $K_1$ | 10 | nM | " | Michaelis constant |
| V2 | $V_2$ | 0.25 | $nM^{-1}.s^{-1}$ | " | Maximal enzyme rate |
| KK2 | $K_2$ | 8 | nM | " | Michaelis constant |
| k3 | $k_3$ | 0.025 | $s^{-1}$ | " | Catalytic rate constant |
| KK3 | $K_3$ | 15 | nM | " | Michaelis constant |
| k4 | $k_4$ | 0.025 | $s^{-1}$ | " | Catalytic rate constant |
| KK4 | $K_4$ | 15 | nM | " | Michaelis constant |
| V5 | $V_5$ | 0.75 | $nM^{-1}.s^{-1}$ | " | Maximal enzyme rate |
| KK5 | $K_5$ | 15 | nM | " | Michaelis constant |
| V6 | $V_6$ | 0.75 | $nM^{-1}.s^{-1}$ | " | Maximal enzyme rate |
| KK6 | $K_6$ | 15 | nM | " | Michaelis constant |
| k7 | $k_7$ | 0.025 | $s^{-1}$ | " | Catalytic rate constant |
| KK7 | $K_7$ | 15 | nM | " | Michaelis constant |
| k8 | $k_8$ | 0.025 | $s^{-1}$ | " | Catalytic rate constant |
| KK8 | $K_8$ | 15 | nM | " | Michaelis constant |
| V9 | $V_9$ | 0.5 | $nM^{-1}.s^{-1}$ | " | Maximal enzyme rate |
| KK9 | $K_9$ | 15 | nM | " | Michaelis constant |
| V10 | $V_{10}$ | 0.5 | $nM^{-1}.s^{-1}$ | " | Maximal enzyme rate |
| KK10 | $K_{10}$ | 15 | nM | " | Michaelis constant |

Notes: In some cases, parameter symbols were altered to accommodate specific conventions in the modeling software used to implement the model. Some parameters were ultimately adjusted to fit specific data sets.

### 3.3 Sensitivity Analysis

In order to explore the relative importance of specific model parameters for LF potency, we conducted a preliminary model-based sensitivity analysis. In particular, we compared the relative importance of the combined pore transport parameter $P_{max}q_{max}$ and the cytosolic half-life of LF on the cytosolic LF concentration (and hence on MAPKK cleavage and signaling disruption).

In general, the sensitivity $S$ of $LF_c$ to a particular parameter parameter $P$ (at time $t$) is given by:

$$S = \partial LF_c / \partial P \quad \text{Equation 8}$$

To compare sensitivity of $LF_c$ to different parameters $P$, one needs to normalize with respect to $P$:

$$S_N = \partial LF_c / (\partial P / P_0) = P_0 . \partial LF_c / \partial P \quad \text{Equation 9}$$

To estimate a fully normalized sensitivity parameter which is independent of the size of the output $LF_c$ we also need to normalize with respect to $LF_c$ (at each time point):

$$S_A = [P_0 / LF_c\ (t)] . \partial LF_c / \partial P \quad \text{Equation 10}$$

## 4.0 RESULTS

### 4.1 Parameter Estimates

We have previously applied the first order rate equations to a variety of data in order to estimate the rate constants *KX* (Robinson *et al.*, 2010). The results of this analysis are given in Table 2 below. The experiments of Pelizzari *et al.* (1999) and Muehlbauer *et al.* (2007) are *in vitro* studies in which PA is in excess, and we may assume that $LF_c$ is determined by $LF_e$, the LF concentration in the surrounding medium. In such cases, we may improve somewhat on this simple analysis by assuming an "effective" second-order rate constant, $KX2_{eff}$, which can be calculated by dividing the fitted *KX* value by $LF_e$. Such calculated values for $KX2_{eff}$, which take into account, albeit crudely, the different LF concentrations in the medium (Robinson *et al.*, 2010) are also given in Table 2. Values of $KX2_{eff}$ thereby provide a better indication of the sensitivity or susceptibility of the particular macrophage type to LF than do values for *KX*.

**Table 2. Rate Constants KX and $KX2_{eff}$ for the Interaction of Specific Combinations of LF and PA with Various Macrophage Cell Types *In Vitro***

| Macrophage Type/Source | $LF_e$ Concentration (ng/mL) | $PA_e$ Concentration (ng/mL) | KX ($s^{-1}$) (fitted) | $KX2_{eff}$ $(ng/ml)^{-1}$ $s^{-1}$§ | Data Reference |
|---|---|---|---|---|---|
| RAW264.7 | unk. | unk. | $2.9 \times 10^{-4}$ | - | Gutting *et al.*, 2005 |
| J774A.1 | unk. | unk. | $1.2 \times 10^{-4}$ | - | Gutting *et al.*, 2005 |
| RAW264.7 | 200 | 200 | $2.0 \times 10^{-4}$ | $1.0 \times 10^{-6}$ | Pellizzari *et al.*, 1999 |
| BALB/C | 250 | 500 | $4.5 \times 10^{-4}$ | $1.8 \times 10^{-6}$ | Muehlbauer *et al.*, 2007 |
| C3H | 250 | 500 | $4.5 \times 10^{-4}$ | $1.8 \times 10^{-6}$ | Muehlbauer *et al.*, 2007 |
| AKR | 250 | 500 | $1.0 \times 10^{-5}$ | $4.0 \times 10^{-8}$ | Muehlbauer *et al.*, 2007 |
| BL/6* | 250 | 500 | $1.2 \times 10^{-5}$ | $4.8 \times 10^{-8}$ | Muehlbauer *et al.*, 2007 |
| DBA | 250 | 500 | $1.4 \times 10^{-5}$ | $5.6 \times 10^{-8}$ | Muehlbauer *et al.*, 2007 |
| Human | 250 | 500 | $1.1 \times 10^{-5}$ | $4.4 \times 10^{-8}$ | Muehlbauer *et al.*, 2007 |

Notes: Since the molecular weight (MW) of LF is ~ 90 kDa, concentrations of 200 and 250 ng/ml correspond to 2.2 and 2.8 nM respectively; the MW of PA is 83kDa, so 200 and 500 ng/mL correspond to 2.4 and 6.0 nM (from Robinson *et al.*, 2010). *Two separate experiments with BL/6 derived macrophages were reported; unk = unknown; §An effective second order rate constant (calculated as $KX/LF_e$, see Discussion and Conclusions)

Although such an analysis goes some way towards acknowledging the effect of local LF concentrations on MAPKK cleavage, in the present paper we explicitly model the accumulation of LF in the cytosol, which we assume is governed by Equations 6 and 7. It thus depends on a number of parameters (see above, and Table 1). Note that only four largely unknown or poorly determined parameters ($KX2$, $R$, $K_m^{LF}$, $K_m^{PA}$) determine the cytosolic LF concentration. The binding affinities $K_m^{LF}$ and $K_m^{PA}$ are determined within limits (Table 1), lying within the range $K_m^{PA} = 0.01$ nM, $K_m^{LF} = 0.4$ nM; and $K_m^{PA} = 0.4$ nM, $K_m^{LF} = 11$ nM. We are thus left with two parameters as unknowns: the cleavage rate constant $KX2$, and the composite parameter $R$ determined by the product of the total number of receptor sites (per cell) and the maximum transport rate of LF by each fully formed "pore" on the cell surface (divided by the cytosolic volume of distribution). We explore the influences of these parameters (under both low and high binding affinity conditions) as they relate to the experimental *in vitro* conditions in Table 2 in the simulations which follow.

The overall behavior of the model is illustrated in Figure 5a and 5b. In each case, the smooth (green) line represents the increase in cytosolic LF according to the model. The oscillating curve represents the MAPK signaling output (double phosphorylated MAPK, MAPKPP). The oscillations are due to the feedback loop in which the MAPKPP output inhibits the initial phosphorylation step in the Kholodenko model (Figure 3). The broken line represents the time-weighted average of this signaling output, which is assumed to be an indicator of its viability, and hence of the viability of the cell as a whole. It is fitted as close as possible to the

experimental cell viability data, in this case the viability of BALB/C and human macrophages in the presence of 250 ng/mL LF and 500 ng/mL PA (Muehlbauer *et al.*, 2007). See Robinson *et al.* (2010) for a more detailed description of the procedure for fitting the model to the experimental data of both Pellizzari *et al.* (1999) and Muehlbauer *et al.* (2007).

In order to tease out the respective influences of the influx parameter *R* and the cleavage rate constant *KX2* on cell viability, we explored the behavior of the model under some informative limiting conditions. If we focus first on LF accumulation in the cytosol, we find that in general, influx is balanced by both interaction with MAPKK and degradation. The final concentration, however, is determined by a balance of influx and degradation. If we set *KX2*=0, we see just this behavior as the curve approaches an asymptote from the origin (see Figure 6, curve a).

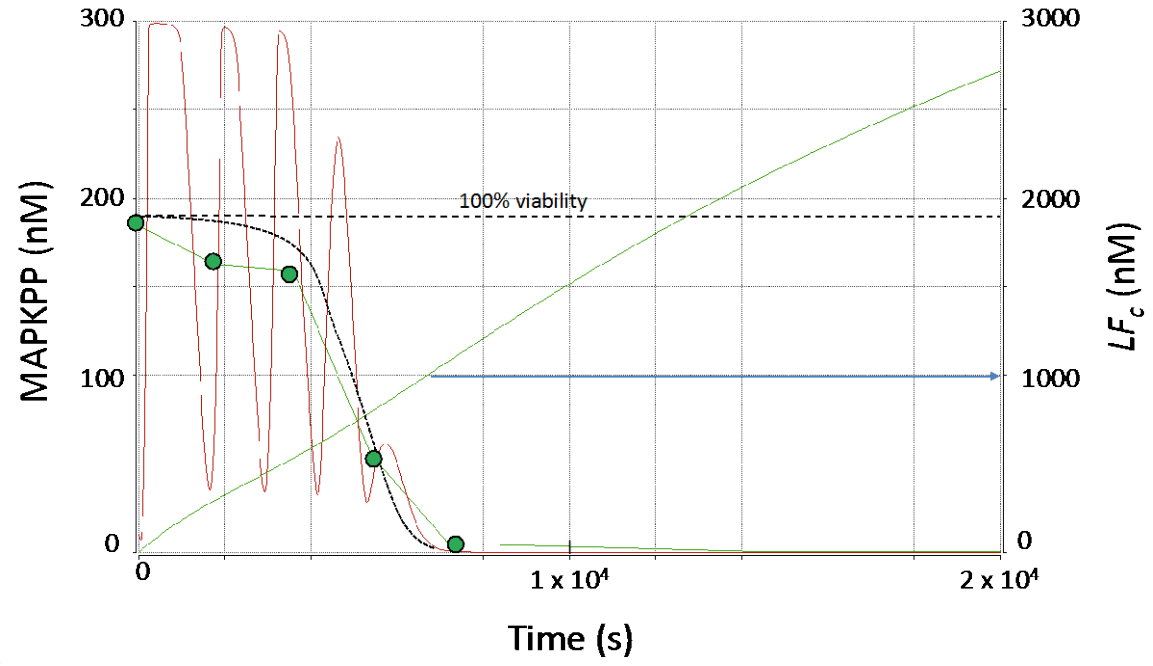


A

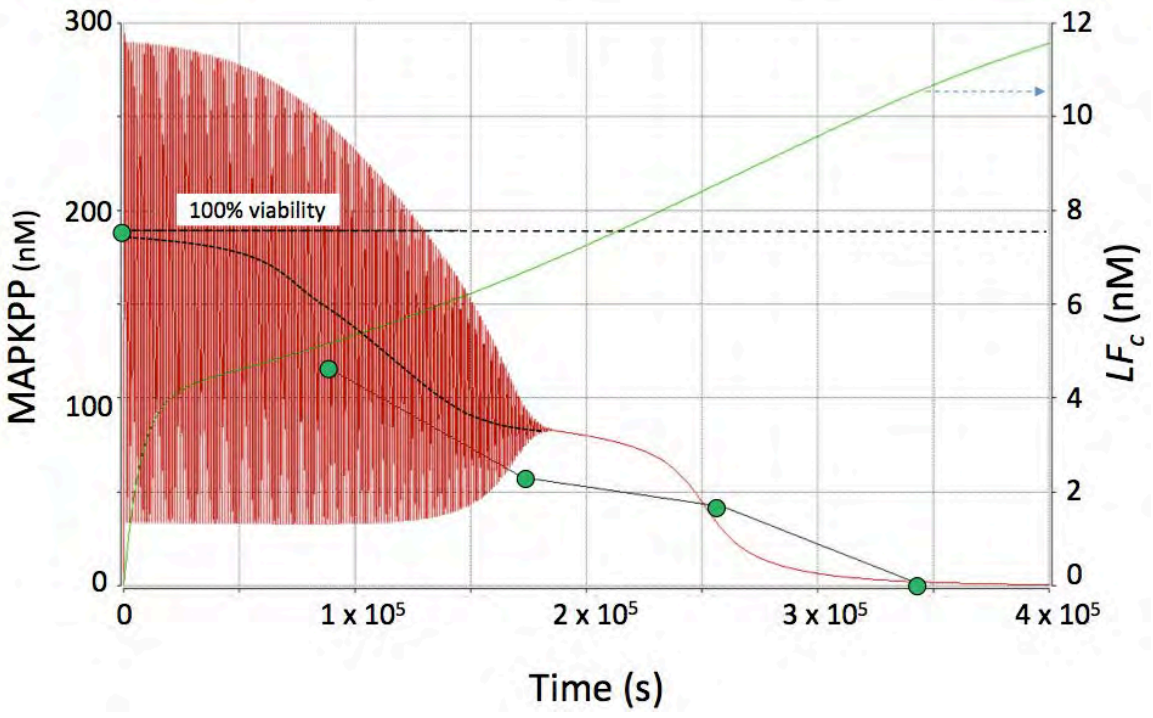


B

**Figure 5. Comparison of MAPK Model Predictions and BALB/C Mouse or Human Macrophage Viability *In Vitro*.** (A) Figure shows the accumulation of LF in the cytosol of the macrophage predicted by the model (green line, RH axis), together with its effect on MAPK signaling (MAPKPP, black line, LH axis). Broken line indicates average MAPKPP levels across multiple cycles. In this case, the external LF concentration LFe is assumed to be 2.8 nM, equivalent to about 250 ng/mL (MW of LF ~ 90 kDa), while $PA_e$ is 6.0 nM, or 500 ng/ml. Also,

$K_m^{PA}$ = 0.01 nM, $K_m^{LF}$ = 0.4 nM, corresponding to high affinity binding of both PA and LF. Note that in this case the "death" of the cell, as indicated by the diminution of the signal, occurs at LF cytosolic concentrations LFc of approximately 1000 nM in our model (blue line, RH axis). Decline in MAPKPP is fitted to data points (Robinson *et al.*, 2010) for BALB/C cells from Muehlbauer *et al.* (2007) (green circles). Data points represent absorbance values at 570 nm following the MTT assay. Fitted values are KX2 = 10-6 $nM^{-1}s^{-1}$ and R = 0.21 nM $s^{-1}$. (B) Human macrophages (green circles) (Muehlbauer *et al.*, 2007), are much more sensitive to the effects of LF than the BALB/C cells in Figure 5a. Signals represent absorbance values at 570 nm following MTT assay. Here cell "death", as indicated by the diminution of the signal (corrected for residual absorbance of dead cells of 30 percent), occurs at LF cytosolic concentrations $LF_c$ of approximately 10-11 nM in our model (blue dotted line, RH axis). In order to capture the early diminution of cell viability, the initial MAPKK concentration has been reduced in the model from 280 nM (Kholodenko, 2000) to 75 nM. Fitted values are KX2 = $10^{-6}$ $nM^{-1}s^{-1}$ and R = 6 x $10^{-4}$ nM $s^{-1}$. (If the initial MAPKK concentration was kept at 280 nM, the fitted R-value would need to be correspondingly larger to fit the data – see Table 3).

For very large values of *KX2*, accumulation of LF in cytosol is negligible until MAPKK is depleted, at which time point, designated by $T_0$, $LF_c$ also ascends to its asymptote (Figure 6, curve b). The time $T_0$ is determined by the ratio of LF influx to the amount of MAPKK available for cleavage, and does not depend on *KX2* (as long as *KX2* is sufficiently large). In fact, for sufficiently large values for $K_m^{LF}$ and $K_m^{PA}$, $T_o$ = *[MAPKK]/R*, where *[MAPKK]* is the total (phosphorylated and unphosphorylated) MAPKK concentration. From Kholodenko (2000), [MAPKK] = 300 nM, so $T_0$ = 300/*R*. While the parameters associated with the MAPK pathway (including initial values for the concentrations of the components, such as MAPKK) are taken from Kholodenko (2000), the influx rate of LF is given by the lumped parameter R (as well as the affinities, $K_m^{LF}$ and $K_m^{PA}$, and the external PA and LF concentrations).

For intermediate values of *KX2*, the behavior is shown in Figure 6, curve (c). In this case, $LF_c$ initially is determined by the relative magnitude of influx versus MAPKK cleavage. After a time (again ~ $T_0$), this transitions smoothly to a balance between influx and degradation as MAPKK is depleted. As we shall see, $T_o$ roughly coincides with the time at which LF exposed cells lose their viability, thus allowing an estimate of R to be made.

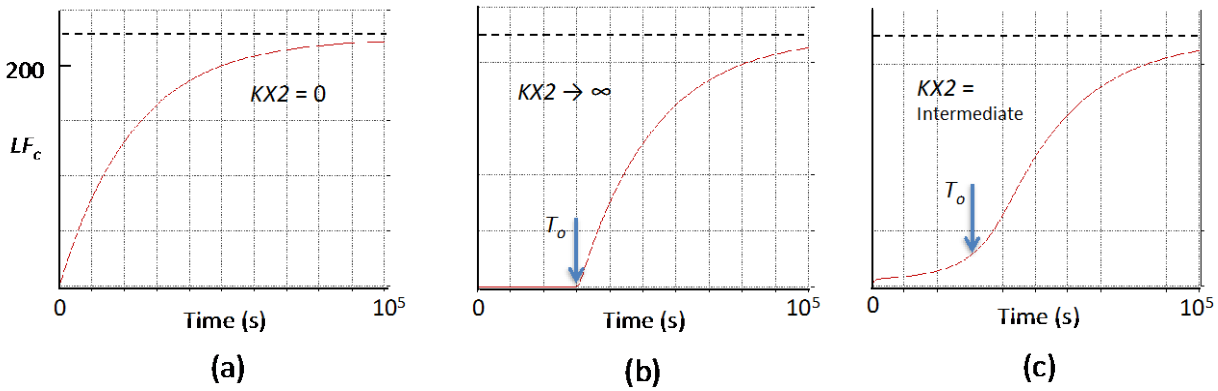


**Figure 6. Simulations of LF Accumulation in the Cytosol under Different Hypothetical MPAKK Cleavage Conditions.** Broken line represents steady-state in which influx equals removal of LF from the cytosol. $T_0$ represents time by which MAPKK is essentially depleted, and removal is by degradation alone.

All this occurs of course as MAPK signaling is disrupted and cell viability is compromised. The degree of disruption is determined both by the cytosolic LF concentration together with the magnitude of the cleavage rate constant *KX2*. At critical early times, $LF_c$ is determined largely by the influx rate parameter *R* (as discussed above), so MAPK signaling disruption is essentially the result of the combined effects of the unknown parameters *KX2* and *R*: the same degree of disruption (and hence cell viability, as determined by the experimental data) can be obtained by simultaneously increasing *R* and decreasing *KX2* (or vice versa). The differential susceptibilities of different cell types to LF exposure *in vitro*, shown as $KX2_{eff}$ values in Table 2, are thus potentially due to differences in either influx capacities *R*, or true cleavage rate constants *KX2*, or both. Figure 7 illustrates this – each line represents pairs of R, KX2 values that give the same reduction in MAPK signaling by a certain time (in this case a 50 percent reduction in signaling by 2.5, 5, 20 and 60 hours, respectively).

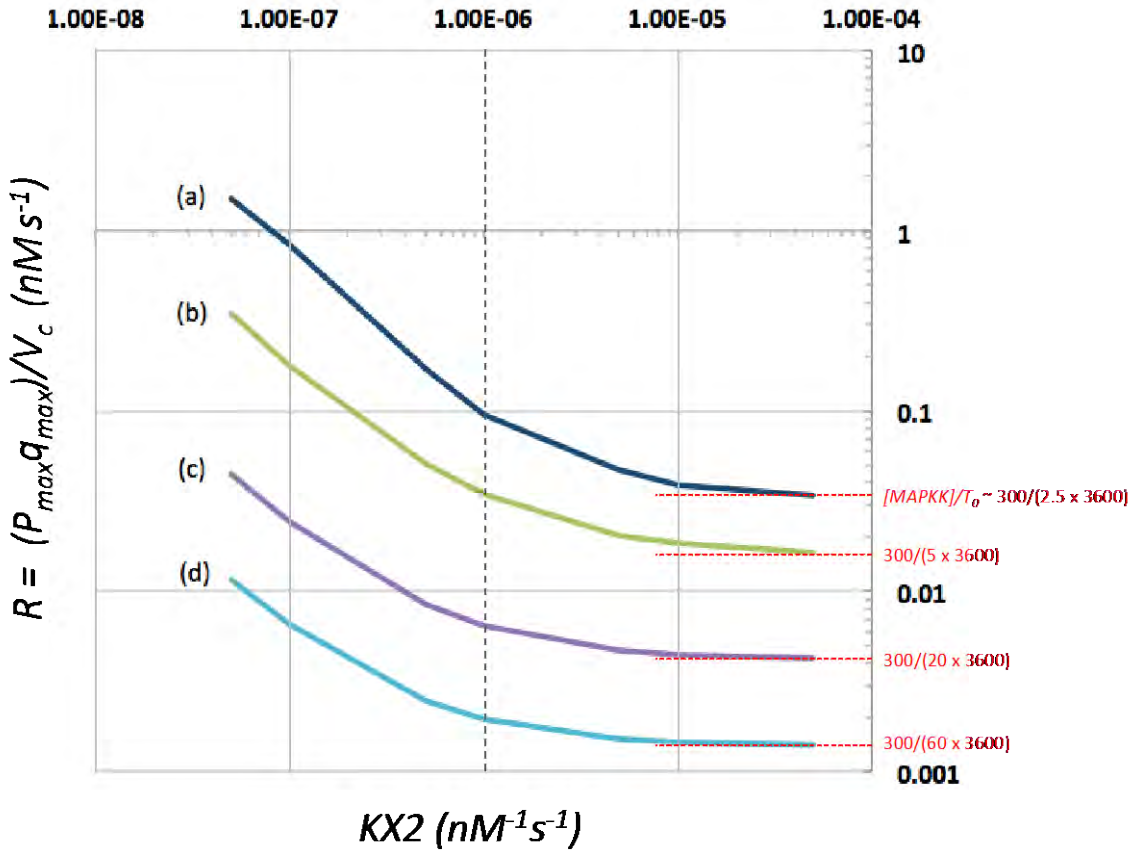


**Figure 7. Calculated Model-Based Values of $KX_2$ and R for Time-Courses of Reductions in MAPK Signaling Output.** Each line indicates a 50 percent reduction at (a) 2.5, (b) 5, (c) 20, and (d) 60 hours. Note that R approaches [MAPKK]/$T_0$ as $KX_2$ becomes large, that [MAPKK] = 300 nM, and that $T_0$ can be approximated by this time to 50 percent reduction in signaling output (red dotted line). Other parameters are $PA_e$ = 6.0 nM, $LF_e$ = 2.8 nM, $K_m^{PA}$ = 0.1 nM, and $K_m^{LF}$ = 4 nM.

In order to estimate lumped influx parameters and cleavage rate constants for various cell types exposed to anthrax LF and PA *in vitro*, we fit the available *in vitro* cell viability data by assuming again (Robinson *et al.*, 2010) that the reduction in output of the MAPK pathway (MAPKPP in Figure 3) as a result of cytosolic LF-induced cleavage of MAPKK is correlated with reductions in macrophage viability. Since cleavage is the result of both transport of LF into the cytosol (determined by *R*) and the cleavage rate constant *KX2*, and since variations in susceptibility is more likely due to differences in the transport parameters, particularly receptor density (which may vary over almost two orders of magnitude for different cell types (Abi-Habib, 2005; Fleming *et al.*, 2009)), we assume a common (arbitrary) value for *KX2* ($10^{-6}$ $nM^{-1}s^{-1}$), and fit *R* by eye to each study in Table 2 for which the concentrations of LF and PA in the bathing medium are available. Note, we do this for the extreme values of the binding affinities $K_m^{LF}$ and $K_m^{PA}$ (see Table 1), with values $K_m^{PA}$ = 0.01 nM, $K_m^{LF}$ = 0.4 nM (high affinity); and $K_m^{PA}$ = 0.4 nM, $K_m^{LF}$ = 11 nM (low affinity) respectively. The results are shown in Table 3.

Note that fitting of the Muehlbauer *et al.* (2007) data for the AKR, BL/6, DBA and human macrophages is very approximate since the model predicts a much sharper decline in MAPK signaling output than is reflected in the cell viabilities for these less sensitive cell types. The sharpness can be reduced by reducing the initial supply of MAPKK in the system (and simultaneously reducing R or KX).

**Table 3. Fitted Values for the Ratio $R = (P_{max}q_{max})/V_c$ ($nM\,s^{-1}$) for the Interaction of Specific Combinations of LF and PA with Various Macrophage Cell Types *In Vitro***

| Macrophage Type/Source | LF Conc. (nM) | PA Conc. (nM) | Fitted R value ($nM\,s^{-1}$) Low affinity | Fitted R value ($nM\,s^{-1}$) High affinity[§] | Data Reference |
|---|---|---|---|---|---|
| RAW264.7 | 2.2 | 2.4 | $1.3 \times 10^{-1}$ | $8.0 \times 10^{-2}$ | Pellizzari *et al.*, 1999 |
| BALB/C | 2.8 | 6.0 | $3.2 \times 10^{-1}$ | $2.1 \times 10^{-1}$ | Muehlbauer *et al.*, 2007 |
| C3H | 2.8 | 6.0 | $3.5 \times 10^{-1}$ | $2.3 \times 10^{-1}$ | Muehlbauer *et al.*, 2007 |
| AKR | 2.8 | 6.0 | $2.4 \times 10^{-3}$ | $1.6 \times 10^{-3}$ | Muehlbauer *et al.*, 2007 |
| BL/6* | 2.8 | 6.0 | $2.7 \times 10^{-3}$ | $1.8 \times 10^{-3}$ | Muehlbauer *et al.*, 2007 |
| DBA | 2.8 | 6.0 | $2.7 \times 10^{-3}$ | $1.8 \times 10^{-3}$ | Muehlbauer *et al.*, 2007 |
| Human | 2.8 | 6.0 | $2.4 \times 10^{-3}$ | $1.6 \times 10^{-3}$ | Muehlbauer *et al.*, 2007 |

Notes: The cleavage rate constant KX2 for each cell type was assumed to be the same (and equal to $10^{-6}$ $nM^{-1}s^{-1}$).
[§]Values for the affinities PA and LF for their respective binding sites were assumed to be at the lower and upper ends of their measured ranges, respectively; *Two separate experiments with BL/6 derived macrophages were reported.

## 4.2 Sensitivity Analysis

The sensitivity $S_A$ of cytosolic LF concentration $LF_c$ to influx parameter $P_{max}q_{max}$ and to the degradation (outflux) parameter *TH,* the half-life of LF in the cytosol, according to Equation 11, are shown in Figure 8. At early times after exposure to LF, $LF_c$ (and therefore attenuation of MAPK signaling) is driven primarily by influx of LF to the cytosol, rather than degradation half-life. At later times (after about $4 \times 10^4$ s or about half a day), however, the cytosolic half-life TH assumes equal influence on $LF_c$.

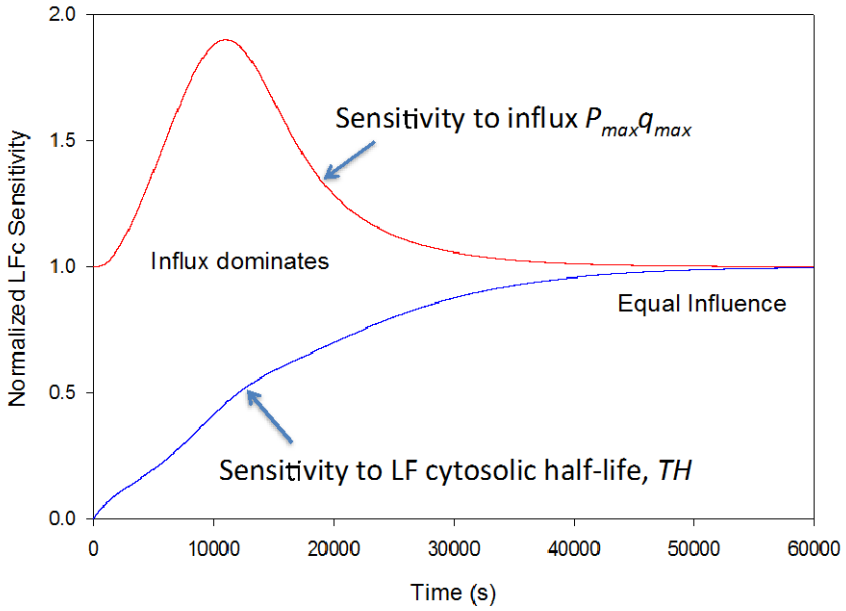


**Figure 8. Sensitivity Analysis of Cytosolic LF Concentration to Influx Parameter and to the Half-Life of LF in the Cytosol.** The sensitivity $S_A$ of cytosolic LF concentration $LF_c$ to influx parameter $P_{max}q_{max}$ (top curve) and to the degradation (outflux) parameter TH, the half-life of LF in the cytosol (lower curve), according to Equation 11. Initially, the influx parameter dominates the determination of $LF_c$, whereas at later times (after about 4 x $10^4$ s), influx and outflux parameters share influence.

## 5.0 DISCUSSION

The present model describes aspects of the interaction between BA and the early responder cells, the alveolar macrophages of the host system. It provides an initial description of the effect of the release of anthrax toxins, specifically LF and PA, on a particular biochemical pathway in the macrophage – the MAPK signaling pathway. As such, it provides a framework for understanding the impact of anthrax on the host system and how the host system's defense mechanisms are disrupted for the benefit of the invading organism. There are likely additional effects of lethal toxin on the host system, such as Nlrp1b cleavage in macrophage pyroptosis (Hellmich *et al.*, 2012). This initial interaction between LF and the MAPK pathway, however, in the context of a specific exposure scenario, is critical in determining BA proliferation and the response of the host's immune system (including macrophage viability and immune cell recruitment). This in turn determines the overall course of the infection, the final impact on the target tissues and the overall health outcome. Specifically, our model describes a critical step in this process: the PA-mediated accumulation of LF in the macrophage cytosol, and its effect in disrupting the host cell's MAPK signaling pathway, leading to cell death. Cytosolic LF accumulation may result from release of LF by endocytosed and germinated spores, or, later in the infection process, directly from LF in the systemic circulation. The current model is a first step: limited data are as yet available for in the development of a fully parameterized and validated model of these processes.

In modeling the interaction of LF with the MAPK pathway of the host cells, we have adopted a specific model for the MAPK pathway, that of Kholodenko (2000). In order to apply this model to the interaction of host immune cells with BA, it was necessary to modify it by including LF-induced cleavage of MAPKK intermediates. In our previous paper (Robinson *et al.*, 2010) we discussed the potential effects of choosing a different model for the MAPK signaling pathway itself. We noted that this question had been explored in detail by Schneider (2008), who modified three published MAPK models to reflect this signal inhibition and to estimate a first-order reaction rate by fitting the models to the data of Gutting *et al.* (2005) for the interaction of BA with RAW264.7 and J774A.1 macrophages. These fitted models were the "ultrasensitivity" model of Huang and Ferrell (1996), the "negative feedback" models of Kholodenko (2000), and the "scaffold protein" model of Levchenko *et al.* (2000). The results showed that the estimated first order rate constants were consistent between the models for each macrophage type. It is to be expected that such robustness with respect to the specific details of the MAPK model would extend to the present more detailed analysis as well. In addition, as Duesbery *et al.* (2001) and others have shown, there is a degree of heterogeneity among the MAPKKs. However, we believe that our representative model, interpreted as a proof-of-concept, captures the essentials of the LF-induced cleavage process, and parameters such as the fitted cleavage rate constants, represent an average or effective parameter value for what in reality is a more complex process.

For simplicity, we have developed the model to describe a situation in which macrophages of various types are exposed to specific concentrations of LF and PA *in vitro*. When such a scenario has been set up experimentally with different macrophage cell types, differences in macrophage survival times were noted (Pellizzari *et al.*, 1999; Muehlbauer *et al.*, 2007). It was assumed, in our model, that the variation in sensitivity to LF exposure was due to variations in the LF transport/endocytosis parameter $R = (P_{max}q_{max})/V_c$ (Table 3), while the biochemical parameter *KX2* representing MAPKK cleavage was assumed to be the same across cell types (= $10^{-6}$ $nM^{-1}s^{-1}$). This assumption is consistent with the observation that receptor densities for PA binding to cells of different types vary from 2,600 receptors/cell for heart to 240,000 receptors/cell for kidney (Abi-Habib, 2005; Fleming *et al.*, 2009). In addition to KX2 and R, values for the affinity constants $K_m^{PA}$ and $K_m^{LF}$ also affect model predictions of cell viability, and Table 1 shows the effect of assuming values at the high and low ends of their measured range. Fitted *R*-values (and so possibly PA receptor densities) for the macrophages in Table 1 range from o.0016 (AKR and human macrophages) to 0.35 nM $s^{-1}$ (C3H macrophages), with smaller values indicative of lower receptor densities and hence lower susceptibility to LF.

It should be noted that additional processes may be involved in the transfer of LF into the cytosol, and that the process may be more complicated than outlined here. For example, recently evidence has emerged to suggest that during BA infection, circulating [$PA_{83}$] may be cleaved by serum proteases, resulting in the free assembly of [$PA_{63}$] heptamers in the serum. These may then associate with circulating LF to form LeTx in the circulation. Vuyisich *et al.* (2012) have also shown that LeTx formed in this way has a higher affinity for cell surface receptors, and may thus be a significant source of cytosolic LF, particularly in later stages of infection. In addition, the connection between PA and LF, the formation of pores, pH effect, etc. needs to be explored in more detail. Detailed mechanisms, such as the pH-dependent tandem Brownian ratchet translocation mechanism for LF of Collier

and co-workers (Krantz *et al.*, 2006), may need to be incorporated more fully into the model. In addition, a completely different mechanism for the release of LF into the cytosol may be involved, involving the disruption of the endosomal membrane (Nablo *et al.*, 2013).

Clearly, in the current model, a number of parameters associated with pore formation, pore transport, as well as biochemical parameters associated with MAPK signaling and its disruption, combine to determine the potency of LF for a host cell. The most important determinants may be different at early and late times following exposure. For example, Gupta *et al.* (2008) speculate that the cytosolic stability of LF is a major determinant of its potency. However, a sensitivity analysis based on our current model shows that initially, the influx parameter dominates the determination of $LF_c$, whereas at later times (after about $4 \times 10^4$ s or about 11 hours), influx and outflux parameters share influence. Hence, in Table 2 above, the cytosolic half-life of LF, *TH,* may be an important factor in the sensitivity of AKR, BL/6, DBA and human macrophages to LF (with their viability half-lives of 48 to 72 hours), but not the RAW264.7, J774A.1 or BALB/C macrophages with their much shorter half-lives of 1-3 hours, where the influx parameter $R$ dominates.

The present model can be used to predict the effect of specific therapeutic interventions. As noted above, at early times after macrophage exposure to LF, influx dominates the cytosolic LF concentration, and even at later times, still shares its influence with the cytosolic half-life of LF. Therefore, small molecules that bind to the PA heptamer are predicted to be more effective in reducing virulence than efforts made to enhance LF degradation. For example, binding of chloroquine and related compounds have been studied (Orlik *et al.*, 2005; Beitzinger *et al.*, 2013). Translocation of the enzymatic components of anthrax-toxin across the endosomal membrane of target cells and channel formation by the heptameric/octameric PA63 binding/translocation component are related phenomena; blocking these channels should also block LF uptake. In our model, this would be reflected in a (blocker concentration-dependent) reduction in the number $P$ of pores available to transport the LF into the cytosol. Chloroquine, and some 4-aminoquinolones, block the PA63-channel in a dose dependent way; several of these compounds have been shown to reduce J774A.1 macrophage lysis by about 50 to 80 percent, and enhance cell viability *in vitro* (Orlik *et al.*, 2005). Half-saturation constants for chloroquine and related compounds range from 0.0013 mM to 2 mM (Orlik *et al.*, 2005), compared with $K_m^{LF}$ values for LF translocation of 0.4 to 11 nM (Elliott *et al.*, 2000).

Our current model is just a beginning in what we envisage to be an ongoing process of iterative model development. It therefore has a number of limitations. Firstly, the model in its current state is over-parameterized. In order to fully validate the model, we need independent measurements of several key parameters, such as the maximum number of pores, $P_{max}$, able to be formed on the endosome surface and the maximum flux rate per pore, $q_{max}$. However, a model such as the current one, based on the underlying biology and physiology, would be expected to be robust in the sense that it can be used to make predictions with respect to biological variation and a changing environment.

Secondly, as in our previous paper, we have focused on LF, not taking into account the effect of EF on the cellular machinery of the macrophage. EF acts as a calcium anion and calmodulin dependent adenylate cyclase that greatly increases the level of cyclic AMP in the cell. This

increase in cyclic AMP upsets water homeostasis, throws the intracellular signaling pathways off balance, and impairs macrophage function, allowing the bacteria to further evade the immune system. It is envisaged that in our final composite model, the effects of EF will also be taken into account. In the present paper, however, we have focused entirely on LF, and have developed our model based on *in vitro* systems in which cells are exposed to various concentrations of LF and PA without the confounding effects of EF. Clearly, however, exposure to BA pathogens (or spores), either *in vitro* or *in vivo,* leads to a situation in which both LF and EF may contribute to cell death, as well as more complicated kinetics for LF (and EF) accumulation in the cytosol.

The model was successful as a proof-of-concept: such an interaction can be modeled down to the molecular level, and results compared quantitatively with gross observations, such as cell viability and death. The present model can be incorporated as a module in a multi-scale model for anthrax infection as a whole. Indeed, such model development is ongoing in our laboratory, and includes deposition of anthrax spores in the respiratory tract, endocytosis by lung macrophages and transport of macrophages to the lymph nodes. We need to compare and combine the transport and proliferation of the key components of this system to give a quantitative framework for disease progression: where do macrophages go in the body, how long does it take to get there compared with the proliferation of anthrax bacteria within them, and at what point are the macrophages killed by the release of toxins within and exposure to toxins without? In addition, this modeling effort requires further studies, designed with parameter validation in mind. Such a comprehensive model will be of ultimate use in risk assessment and in the design and assessment of existing and new therapies, which will be a focus of future work in this area. When combined with the proliferation model that simulates LF dosimetry, and with a description of the biological effect of signal reduction in terms of the cellular response (alterations in gene expression leading to changes in cytokine production, apoptosis etc.), we thus have a model framework that begins to predict the time-course of the biological effects of anthrax exposure in biologically varied individuals. In addition, model predictions can be compared with observations, allowing the model to be validated and, if necessary, modified.

## 6.0 REFERENCES


Abi-Habib RJ, Urieto JO, Liu S, Leppla SH, Duesbery NS, Frankel AE. 2005. BRAF status and mitogen-activated protein/extracellular signal-regulated kinase kinase 1/2 activity indicate sensitivity of melanoma cells to anthrax lethal toxin. Mol Cancer Ther. 4(9):1303-10.

Banks DJ, Barnajian M, Maldonado-Arocho FJ, Sanchez AM, Bradley KA. 2005. Anthrax toxin receptor 2 mediates Bacillus anthracis killing of macrophages following spore challenge. Cell Microbiol. 7(8):1173-85.

Beitzinger C, Bronnhuber A, Duscha K, Riedl Z, Huber-Lang M, Benz R, Hajós G, Barth H. 2013. Designed azolopyridinium salts block protective antigen pores in vitro and protect cells from anthrax toxin. PLoS One. 20;8(6):e66099.

Collier RJ. 2009. Membrane translocation by anthrax toxin. Mol Aspects Med. 30(6):413-22.

Day J, Friedman A, Schlesinger LS. 2011. Modeling the host response to inhalation anthrax. J Theor Biol. 276(1):199-208.

Dixon TC, Meselson M, Guillemin J, Hanna PC. 1999. Anthrax. N Engl J Med. 9;341(11):815-26.
Duesbery NS, Resau J, Webb CP, Koochekpour S, Koo HM, Leppla SH, Vande Woude GF. 2001. Suppression of ras-mediated transformation and inhibition of tumor growth and angiogenesis by anthrax lethal factor, a proteolytic inhibitor of multiple MEK pathways. Proc Natl Acad Sci U S A. 2001 Mar 27;98(7):4089-94.
Duesbery NS, Webb CP, Leppla SH, Gordon VM, Klimpel KR, Copeland TD, Ahn NG, Oskarsson MK, Fukasawa K, Paull KD, Vande Woude GF. 1998. Proteolytic inactivation of MAP-kinase-kinase by anthrax lethal factor. Science. 280(5364):734-7.
Elliott JL, Mogridge J, Collier RJ. 2000. A quantitative study of the interactions of Bacillus anthracis edema factor and lethal factor with activated protective antigen. Biochemistry. 39(22):6706-13.
Fink SL, Cookson BT. 2005. Apoptosis, pyroptosis, and necrosis: mechanistic description of dead and dying eukaryotic cells. Infect Immun. 73(4):1907-16.
Fleming EJ, Hack CE, Robinson PJ, Gearhart JM. 2009. A physiologically based biokinetic (PBBK) model of systemic *Bacillus anthracis* toxins. Poster presentation at Aerobiology in Biodefense III.
Glassman H. 1966. Discussion (Industrial Anthrax). Bacteriol. Rev. 30:657–659.
Guidi-Rontani C. 2002. The alveolar macrophage: the Trojan horse of Bacillus anthracis. Trends Microbiol. 10(9):405-9.
Gupta PK, Moayeri M, Crown D, Fattah RJ, Leppla SH. 2008. Role of N-terminal amino acids in the potency of anthrax lethal factor. PLoS ONE, 3(9):e3130.
Gutting BW, Channel SR, Berger AE, Gearhart JM, Andrews GA, Sherwood RL, Nichols TL. 2008. Mathematically modeling inhalational anthrax. Microbe. 3:78-85.
Gutting BW, Gaske KS, Schilling AS, Slaterbeck AF, Sobota L, Mackie RS, Buhr TL. 2005. Differential susceptibility of macrophage cell lines to Bacillus anthracis-Vollum 1B. Toxicol In Vitro. 19(2):221-9.
Hellmich KA, Levinsohn JL, Fattah R, Newman ZL, Maier N, Sastalla I, Liu S, Leppla SH, Moayeri M. 2012. Anthrax lethal factor cleaves mouse nlrp1b in both toxin-sensitive and toxin-resistant macrophages. PLoS One. 7(11):e49741.
Hill AV. 1910. The possible effects of the aggregation of the molecules of haemoglobin on its dissociation curves. J Physiol. 40:iv–vii.
Huang CY, Ferrell JE Jr. 1996. Ultrasensitivity in the mitogen-activated protein kinase cascade. Proc Natl Acad Sci U S A. 93(19):10078-83.
Jones E, Adcock IM, Ahmed BY, Punchard NA. 2007. Modulation of LPS stimulated NF-kappaB mediated nitric oxide production by PKCε and JAK2 in RAW macrophages. J Inflamm. 4(1):23.
Kholodenko BN. 2000. Negative feedback and ultrasensitivity can bring about oscillations in the mitogen-activated protein kinase cascades. Eur J Biochem. 267(6):1583-8.
Kintzer AF, Thoren KL, Sterling HJ, Dong KC, Feld GK, Tang II, Zhang TT, Williams ER, Berger JM, Krantz BA. 2009. The protective antigen component of anthrax toxin forms functional octameric complexes. J Mol Biol. 392(3):614-29.
Krantz BA, Finkelstein A, Collier RJ. 2006. Protein translocation through the anthrax toxin transmembrane pore is driven by a proton gradient. J Mol Biol. 355(5):968-79.
Kumar R, Chow CC, Bartels JD, Clermont G, Vodovotz Y. 2008. A mathematical simulation of the inflammatory response to anthrax infection. Shock. 29(1):104-11.

Levchenko A, Bruck J. Sternberg WP. 2000. Scaffold proteins may biphasically affect the levels of mitogen-activated protein kinase signaling and reduce its threshold properties. Proc Natl Acad Sci U S A 97(11):5818-23

Liu S, Zhang Y, Moayeri M, Liu J, Crown D, Fattah RJ, Wein AN, Yu ZX, Finkel T, Leppla SH. 2013. Key tissue targets responsible for anthrax-toxin-induced lethality. Nature. 501(7465):63-8.

Luby-Phelps K. 2000. Cytoarchitecture and physical properties of cytoplasm: volume, viscosity, diffusion, intracellular surface area. Int Rev Cytol. 192:189-221.

Muehlbauer SM, Evering TH, Bonuccelli G, Squires RC, Ashton AW, Porcelli SA, Lisanti MP, Brojatsch J. 2007. Anthrax lethal toxin kills macrophages in a strain-specific manner by apoptosis or caspase-1-mediated necrosis. Cell Cycle. 6(6):758-66.

Nablo BJ, Panchal RG, Bavari S, Nguyen TL, Gussio R, Ribot W, Friedlander A, Chabot D, Reiner JE, Robertson JW, Balijepalli A, Halverson KM, Kasianowicz JJ. 2013. Anthrax toxin-induced rupture of artificial lipid bilayer membranes. J Chem Phys. 139(6):065101.

Orlik F, Schiffler B, Benz R. 2005. Anthrax toxin protective antigen: inhibition of channel function by chloroquine and related compounds and study of binding kinetics using the current noise analysis. Biophys J. 88(3):1715-24.

Pellizzari R, Guidi-Rontani C, Vitale G, Mock M, Montecucco C. 1999. Anthrax lethal factor cleaves MKK3 in macrophages and inhibits the LPS/IFNgamma-induced release of NO and TNFalpha. FEBS Lett. 462(1-2):199-204.

Robinson PJ, Fleming EJ, Hack CE, Schneider DJ, Gearhart JM. 2010. Biologically-based modeling of anthrax infection: modulation of macrophage MAPK signaling pathway by lethal toxin. J Med CBR Def. 8.

Schneider DJ. 2008. Three models of anthrax toxin effects on the MAP-kinase pathway and macrophage survival. Thesis, Air Force Institute of Technology, Wright-Patterson AFB, OH.

Scobie HM, Young JA. 2005. Interactions between anthrax toxin receptors and protective antigen. Curr Opin Microbiol. 8(1):106-12.

Segel LA (ed.) 1980. Mathematical Models in Molecular Cellular Biology. Cambridge University Press, New York.

Vitale G, Pellizzari R, Recchi C, Napolitani G, Mock M, Montecucco C. 1998. Anthrax lethal factor cleaves the N-terminus of MAPKKs and induces tyrosine/threonine phosphorylation of MAPKs in cultured macrophages. Biochem Biophys Res Commun. 248(3):706-11.

Vuyisich M, Sanders CK, Graves SW. 2012. Binding and cell intoxication studies of anthrax lethal toxin. Mol Biol Rep. 39(5):5897-903.

Wei W, Lu Q, Chaudry GJ, Leppla SH, Cohen SN. 2006. The LDL receptor-related protein LRP6 mediates internalization and lethality of anthrax toxin. Cell. 124(6):1141-54.

Wigelsworth DJ, Krantz BA, Christensen KA, Lacy DB, Juris SJ, Collier RJ. 2004. Binding stoichiometry and kinetics of the interaction of a human anthrax toxin receptor, CMG2, with protective antigen. J Biol Chem. 279(22):23349-56.

Young JA, Collier RJ. 2007. Anthrax toxin: receptor binding, internalization, pore formation, and translocation. Annu Rev Biochem. 76:243-65.

Zhang Y, Ting AT, Marcu KB, Bliska JB. 2005. Inhibition of MAPK and NF-kappa B pathways is necessary for rapid apoptosis in macrophages infected with Yersinia. J Immunol. 174(12):7939-49.

## LIST OF ACRONYMS

| | |
|---|---|
| AMP | adenosine monophosphate |
| BA | *Bacillus anthracis* |
| DTIC | Defense Technical Information Center |
| DTRA | Defense Threat Research Agency |
| EdTx | edema toxin |
| EF | edema factor |
| HJF | Henry M. Jackson Foundation for the Advancement of Military Medicine |
| LeTx | lethal toxin |
| LF | lethal factor |
| MAPK | mitogen-activated protein kinase |
| MAPKK | MAPK kinases |
| MAPKPP | double phosphorylated MAPK |
| MW | molecular weight |
| NO | nitric oxide |
| PA | protective antigen |
| TLR | toll-like receptor |